Thermal Stresses in the Accessories of Heat Treatment Furnaces vs Cooling Kinetics

A. Bajwoluk*, P. Gutowski

Mechanical Engineering Faculty, West Pomeranian University of Technology, Szczecin
Al. Piastów 19, 70-310 Szczecin, Poland
* Corresponding author. E-mail address: Artur.Bajwoluk@zut.edu.pl

Abstract

Depending on the course of the processes of heat treatment and thermo-chemical treatment, the technological equipment of heat treatment furnaces is exposed to different operating conditions, as the said processes differ among themselves in the temperature of annealing and atmosphere prevailing in the furnace chamber, in the duration of a single work cycle and in the type and temperature of the coolant. These differences affect the magnitude of stresses occurring in each cycle of the operation of furnace accessories, and thus play an important role in fatigue processes leading to the destruction of these accessories. The kinetics of temperature changes during each cooling process plays an important role in the formation of thermal stresses on the cross-section of the cooled parts. It depends on many factors, including the initial cooling temperature, the type and temperature of the cooling medium, or the dimensions and shape of the object. This article presents a numerical analysis of the effect of the initial temperature on the distribution of stresses on the cross-section of the grate ribs, generated in the first few seconds of the cooling process carried out in two cooling media, i.e. hardening oil and water. The analysis was carried out by the finite element method, based on the results of experimental testes of temperature changes in the rib during its cooling.

Keywords: Application of information technology to the foundry industry, Cast grates, Thermal stresses, Heat treatment equipment

1. Introduction

The conditions under which the technological equipment of furnaces for heat treatment and thermo-chemical treatment is operating have a significant impact on the durability of this equipment. A set of unfavorable factors that in subsequent operating cycles affect furnace accessories promotes the development of fatigue processes, and with the elapsing time of the equipment operation it is necessary to withdraw the castings from further use due to the degradation of initially good mechanical properties and the appearance of cracks or large deformations[1-6]

There are many factors that determine the complex character of thermal fatigue in furnace accessories. Among them, an important role play thermal stresses generated in each operating cycle as a result of temperature gradient formed on the cross-section of the heated and cooled part, especially in the vicinity of thermal nodes generated in places with increased wall thickness or between different areas of the tooling [5-9].

Considering the fact that the source of thermal stresses is the uneven temperature distribution in a given element, their occurrence is closely related to the kinetics of the heating and cooling processes to which, together with the charge being transported, are subjected components of the furnace tooling. Especially, fast running cooling processes can lead to high stresses in the accessories, which result in plastic deformations and cracks [5-11]. The course of the cooling kinetics depends on the conditions of the thermal cycle, on the type and temperature of the cooling medium and also on the geometrical parameters of the tooling design, along with the geometry, mass and distribution of the processed charge.

The article presents the results of numerical analysis of the effect of the initial temperature on the thermal stress distribution in a sample whose shape imitates the shape of a vertical rib of the charge transporting grate. The stresses formed during cooling in two cooling media, i.e. hardening oil and water were examined. The temperature distributions on the cross-section of the cooled grate rib, used in the thermal stress analysis, were determined numerically based on the experimentally determined, during given cooling cycles, temperature changes in the sample core.

2. Object of study

Accessories for charge transport in furnaces for heat treatment and thermo-chemical treatment are usually made of creep resistant alloys, especially austenitic stainless steel [1-6,12-14]. Depending on the type of transported charge in the furnace and furnace construction, this equipment can be used in the form of individual grates, multi-level sets or baskets. The choice of a particular design solution and type of material is determined by such factors as the type of heat treatment process, geometrical dimensions of the furnace chamber, the method of charge transport to and from the furnace, and the size, type and distribution of the charge in furnace [6,15,16].
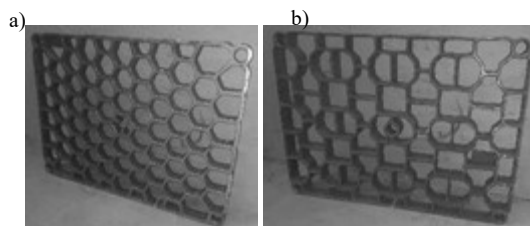

Fig. 1. Examples of accessories for charge transport in furnaces for heat treatment and thermo-chemical treatment

Furnace accessories are usually operated in thermal cycles which promotes the process of thermal fatigue, the more that the accessories are simultaneously exposed to the effect of such factors as high, unevenly distributed and rapidly changing temperature, mechanical load exerted by the transported charge, or carburizing atmosphere. Thermal stresses generated in the tooling construction in each subsequent work cycle are the essential factor contributing to the growth of deformations and development of cracks. Theoretical studies confirmed by practical experience [11] indicate that through changes in the design it is possible to significantly influence the distribution of stresses arising in the tooling life cycle and affect in this way the tooling durability.

In most solutions used in industry, regardless of the form of the entire charge transport set, the heat-treated items rest directly on grates or spacers, which are usually thin-walled castings of an openwork design, manufactured in the shape of a rectangle, square or circle (Fig. 1) [6, 15]. Their basic components are vertical ribs, which together with the interconnections constitute a larger (sometimes total) part of the whole casting. The single rib resembles a rectangular prism with a thickness in the range of 6 ÷ 12 mm, but the grates used most often are those with the wall/rib thickness comprised in the range between 8 ÷ 10 mm.

Due to the elementary nature of the grate wall, to collect information about various mechanisms of stress buildup during the initial phase of the cooling process carried out under different conditions, the results of simulation analysis of stresses generated during cooling of a single vertical rib were used. The input data assumed to determine the thermal stress distribution was obtained from experimental measurements of point temperature changes inside the tested samples during preset cooling cycles.

3. Kinetics of temperature changes in the grate rib during cooling process

The thermal stresses occurring in each cycle of furnace accessories operation are caused, among others, by temperature gradient formed in the heated or cooled part. Due to the fact that it is not physically possible to simultaneously and uniformly change the temperature in the entire volume of this part, its surface and core undergo this change at different rates. Due to the uneven heating and cooling rate, the gradient also arises in the vicinity of thermal nodes in the wall connections and between the regions loaded and unloaded with the charge [5-9, 11].

Temperature differences between the core, the surface and the near-surface zone of the examined element tend to increase especially in the initial moments of the cooling processes, which usually run much more intensively than the heating processes.

To obtain by calculations the values of the distribution of thermal stresses arising in the grate rib during cooling possibly closest to the real values, information on real temperature distribution on the cross-section of the rib during cooling is needed. For this purpose, experimental tests of temperature changes inside the sample shaped like a vertical rib of the grate were carried out as a function of the cooling time. The obtained results were next used to validate temperature change distributions calculated by numerical analysis.

During tests, a rectangular 80x50x8 mm sample (Fig. 2) made from the cast 1.4849 steel (GX40NiCrSiNb38-19) was heated to a preset temperature, and then cooled in a tank in the selected coolant. Holes with a diameter of $\varphi = 1$ mm were drilled to a depth

In the holes, during measurements, K-type thermocouple tips were placed. To avoid unforeseen thermocouple movement during measurement, it was additionally mounted in a special holder attached to the sample. During the test cycle, data from the thermocouple were recorded with an AR205 temperature recorder.

In subsequent measuring cycles, the sample before cooling was heated in the furnace to 300, 500, 700 or 900°C, and then placed in the coolant, which was either OH 70 hardening oil or water. In either case, the temperature of the coolant was in the range of 22 ± 1.5°C. The temperature changes obtained in the sample core in both cooling media are plotted in Figures 3 and 4 as a function of the initial temperature.
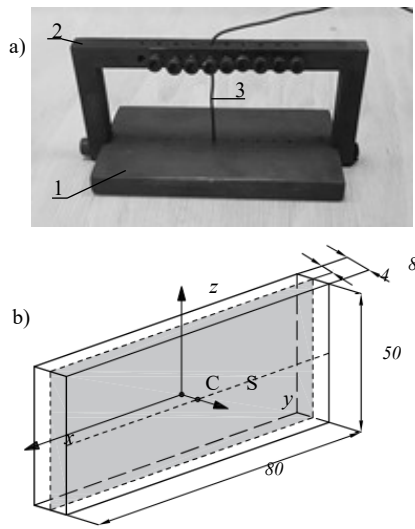
Fig. 2. Test sample a) image of the sample prepared for testing; 1 – sample, 2 – holder, 3 – thermocouple; b) dimensions of the sample of 4 mm in the sample (half of the thickness).
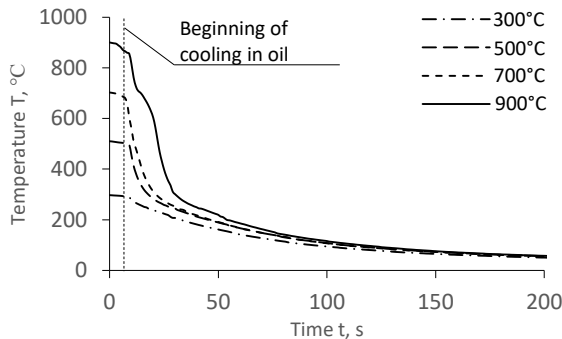

Fig. 3. Temperature changes in the sample core as a function of the cooling time in oil
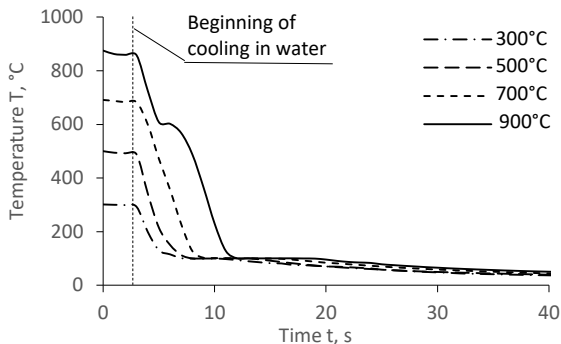

Fig. 4. Temperature changes in the sample core as a function of the cooling time in water

The graphs clearly show (especially for oil cooling) as with the increase in the initial temperature of the heated sample increases the slope of the cooling curve at the beginning of the

process, thus proving its more and more dynamic course. In the case of cooling in water, which is much more intense, the lower limit of 100°C is clearly visible. This is the value above which water is treated as a boiling-evaporating liquid.

The obtained curves were the basis for simulation analysis, the purpose of which was to reproduce numerically the real temperature changes on the cross-section of the cooled part. The calculations were made by the finite element method using a Midas NFX 2014 program. It was assumed in the calculations that the thermal properties of cast 1.4849 steel complied with the EN 10295:2002. *Heat resistant steel castings* standard [17]. It was also assumed that the specific heat of the steel C = 500 J/(kg · K), while its thermal conductivity λ was modelled with a temperature-dependent function (Fig. 5), based on data contained in the above mentioned standard.
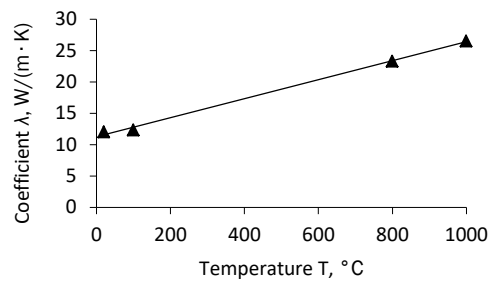

Fig. 5. Thermal conductivity coefficient vs temperature for cast 1.4849

In order to obtain the best compatibility of numerically modelled temperature distributions in the cooled part with data determined experimentally, in the analysis, a variable value [18-20] of the heat transfer coefficient h was assumed. The function shown in Figure 6 was used for cooling in oil.
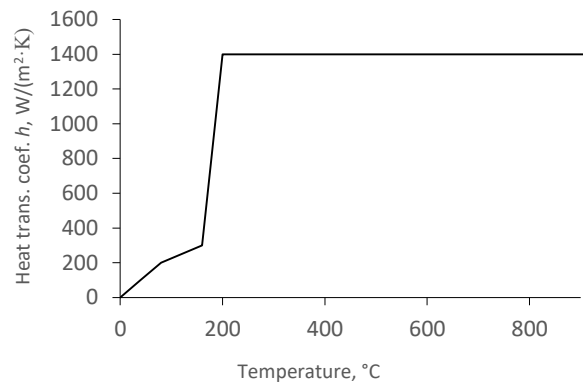

Fig. 6. Heat transfer coefficient vs temperature function adapted for oil

Due to the high initial dynamics of the cooling process in water, and the characteristic slowdown observed at 100°C, it was decided to model water cooling by dividing it into two stages. In the first stage (above 100°C), a constant heat transfer coefficient h of 20000 W/(m2 K) was adapted and an increase in the temperature of the coolant surrounding the sample from initial

22°C to 100°C was assumed. For the second stage - when the temperature inside the sample started dropping again (below 100°C), the average value 1000 W/(m² · K) of this coefficient was assumed.

The graphs determined experimentally and modelled numerically are presented in Figures 7 and 8. Figure 7 shows that in the case of cooling in oil, a very good agreement between the results of experimental tests and numerical calculations was obtained, regardless of the initial temperature of the cooled sample. In the case of cooling in water (Fig. 8), despite a similar course of the obtained function, this agreement was clearly worse. The largest discrepancies were observed in the temperature range from approximately 200°C to 100°C.
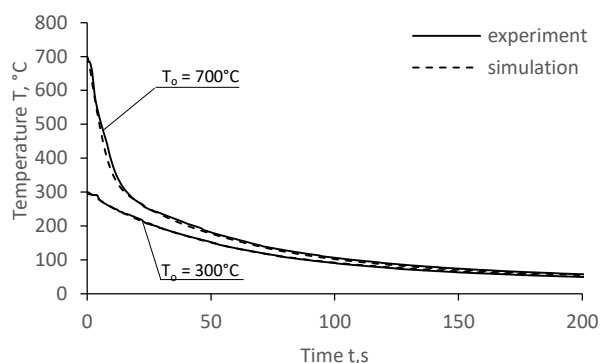

Fig. 7. Comparison of the results of numerical calculations and experimental tests for cooling in oil (22°C) from the initial temperature of 700°C and 300°C
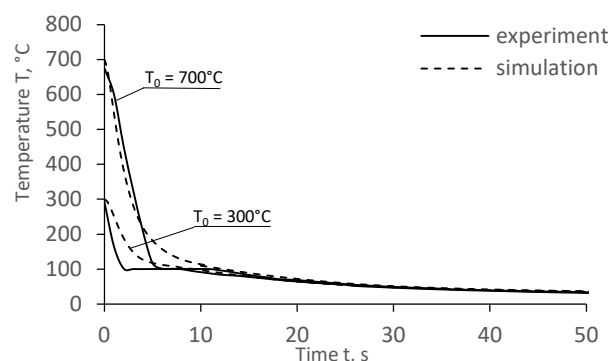

Fig. 8. Comparison of the results of numerical calculations and experimental tests for cooling in water (22°C) from the initial temperature of 700°C and 300°C

The generation of experimentally verified numerical models of temperature distribution on the cross-section of the cooled grate rib for different initial temperatures of cooling and various cooling media was the basis for the analysis of thermal stresses formed on the rib cross-section. In a single rib of the grate, the main source of stress formation is the temperature gradient formed on the cross-section of an element due to the difference in temperature between the near-surface zone and the core. The diagrams in Figures 9 and 10 show changes in this difference

between points S and C (according to the designations in Figure 2) over time, depending on the initial temperature of cooling sample and the type of coolant used. Particularly important information is the period Δt, after which the difference reaches for a given case its maximum value.

From the graphs it follows that in both oil and water cooling, the largest differences in temperature between the core and the surface of the rib occur in the first few seconds that elapse after the part has been immersed in a cooling medium. In the case of water, the differences are much more pronounced than in the case of oil cooling, and they can reach high values even at relatively low values of the initial temperature of the cooled part.
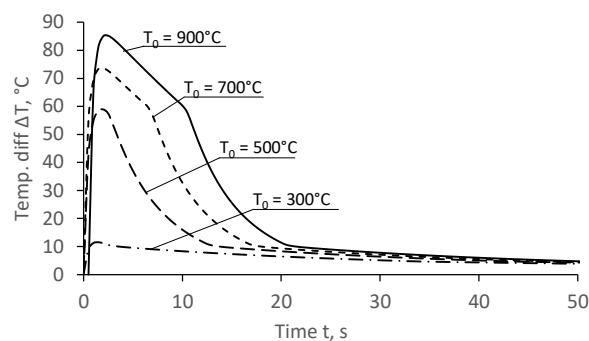

Fig. 9. Difference in temperature between the rib core and surface during cooling in oil
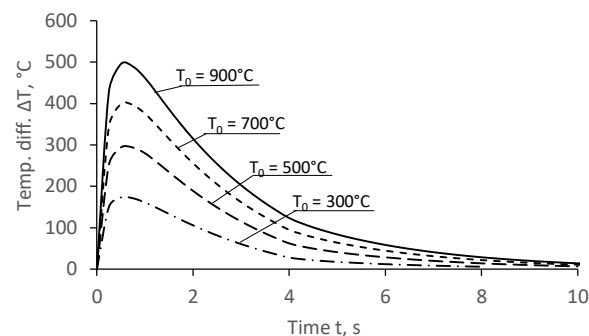

Fig. 10. Difference in temperature between the rib core and surface during cooling in water

4. Analysis of stress distribution

The numerically determined temperature distributions on the cross-section of the cooled element, plotted as a function of the cooling time, were used in the analysis of the thermal stress distribution. In these studies, the load was the change in temperature from uniform in the entire volume of the rib to the distribution which was obtained by numerical calculations at the moment when the difference between the near-surface zone and the core of the sample was the largest.

In the analysis carried out for cast steel, an elasto-plastic nonlinear hardening model was adopted, in which the actual tensile curve was approximated with several straight sections character-rized by different values of the strain-hardening

modulus E_{ai}. In the calculations for austenite, the following empirical data was adopted [8-11]: coefficient of thermal expansion $\alpha = 17.7 \cdot 10^{-6}$ 1/K, Poisson's ratio = 0.253, Young's modulus $E_a = 1.73 \cdot 10^5$ N/mm^2, yield strength $R_{0,2} = 208$ N/mm^2 and the strain-hardening modulus $E_{a1} = 4.09 \cdot 10^3$ N/mm^2 after exceeding the yield point.

Examples of the distribution of directional stresses σ_x and reduced stresses σ_{red} determined after time Δt according to the Huber-Mises yield criterion for cases of cooling in oil and water from the initial temperature of 700°C are shown in Figures 11 and 12, respectively. Analysis of the distribution of directional stresses σ_x after this period (Fig. 11) shows that tensile stresses arise in the near-surface zone, while compressive stresses are formed in the sample core. This is due to the fact that in the first cooling phase, the temperature at the surface changes at a rate much faster than the temperature in the sample core. In this phase, in the near-surface zone, there are larger dimensional changes than in the core, which makes the core undergo the effect of compression upon cooling. This change, in turn, is blocked by the slowly cooling core, which stretches the layers at the surface. If the resulting stresses are strong enough to induce plastic deformation, during further cooling, when this tendency is reversed (the cooling rate is higher in the core than in the near-surface zone), the internal tensile stresses will remain in the core and compressive stresses on the surface.
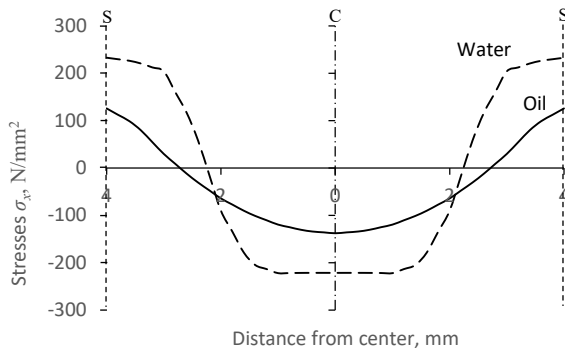

Fig. 11. Distribution of stresses σ_x on the cross-section of the rib after time Δt at cooling from 700°C to 22°C
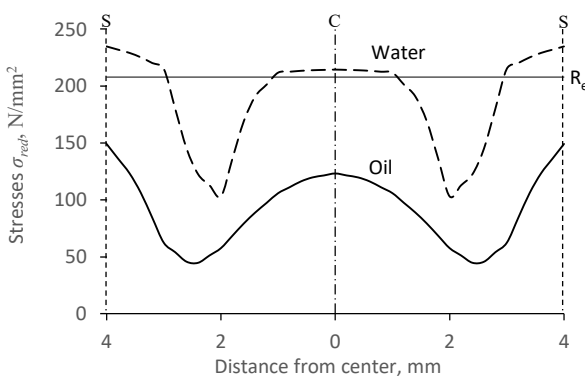

Fig. 12. Distribution of stress σ_{red} on the cross-section of the rib after time Δt at cooling from 700°C to 22°C

From the comparison of reduced stresses σ_{red} distributions on the cross-section of the cooled rib after the time lapse Δt shown in Figure 12, it follows that in the case of water cooling the reduced stresses are much higher and exceed the assumed value of the yield point $R_e = 208$ N/mm^2. In both cases, the highest reduced stresses occur in the near-surface zone of the examined element. The distributions of reduced and directional stresses obtained on the examined direction (C-S) for the two cooling media have very similar shapes. It can be noticed, however, that when the water cooling is more intensive, the point at which the tensile stress changes into compressive is moved away from the surface, which means further extension of the tensile stress zone in this direction.

Figure 13 compares the maximum reduced stresses obtained for the examined cases of cooling in water and oil at different initial temperatures of the cooled part and at the same temperature of the cooling medium. The graphs show that in each case the reduced stresses were higher during cooling in water than during cooling in oil.
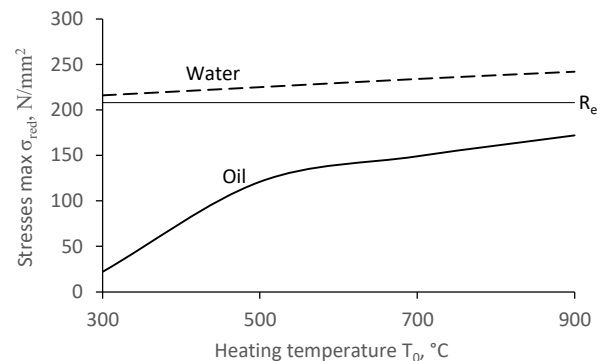

Fig. 13. The maximum reduced stress determined as a function of the initial temperature for cooling in water and oil in 22°C

During cooling in water, the differences between the maximum values of stresses at different initial values of temperature are less pronounced than during cooling in oil. With intensive heat dissipation in water, high stresses which can cause plastic deformation arise even at relatively small temperature differences between the grate rib and coolant, and further increase in this difference does not proportionally increase the maximum stress induced by temperature gradient formed on the cross-section of the wall of the cooled grate rib. With less intensive cooling in oil, up to a value of about 500°C, the increase in the difference between the initial temperature of the grate wall and the cooling medium causes a significant increase in the resulting stresses. However, as the temperature rises, this effect tends to decrease and for high values of the initial temperature of the cooled part, further increase in this temperature does not cause a marked change in stresses

It should be emphasized, however, that actual values of the resulting stresses may differ from those determined by analysis, because temperature changes are accompanied by changes in the mechanical properties of the examined material, in particular by changes in the material constants such as Young's modulus and Poisson's ratio, whose dependence on temperature has not been included in the conducted analysis.

5. Summary

Good agreement between the numerically and experimentally determined changes in temperature distributions suggests that the obtained results of cooling kinetics studies can serve as a basis for the determination of the distribution of thermal stresses generated in the tested parts during cooling process. In the calculations, variable, temperature-dependent, functions of the heat transfer coefficient were used.

Analysis based on the numerically determined changes in temperature distribution over time provided information about the stresses occurring in real walls of the grates under different conditions of the cooling process.

During cooling in a less dynamic medium such as oil, a marked increase in the resulting stresses was observed with an increase in the initial temperature. In the medium in which this process was much more intensive, very strong stresses caused by temperature gradient formed on the cross-section of the examined rib of the grate started arising at a much lower initial temperature, but their further increase with the increase in the initial temperature was less pronounced.

Stronger thermal stresses, exceeding in one cycle the value of yield point, occurring during cooling in water promote faster development of fatigue process in furnace accessories operating under such conditions. This means that the life of these accessories will be much shorter than when the cooling is carried out in less dynamic media.

References

[1] Lai, G.Y. (2007). *High-Temperature Corrosion and Materials Applications*. ASM International.

[2] Davis, J.R. (Ed.). (1997). *Industrial Applications of Heat-Resistant Materials*. In Heat Resistant Materials. ASM International.

[3] Ul-Hamid, et al. (2006). Failure analysis of furnace tubes exposed to excessive temperature. *Engineering Failure Analysis.* 13(6), 1005-1021. DOI: 10.1016/j.engfailanal.2005.04.003.

[4] Reihani, Ali. et al.(2013). Failure analysis of welded radiant tubes made of cast heat-resisting steel. *Journal of failure Analysis and Prevention*. 13(6). DOI: 10.1007/s11668-013-9741-y.

[5] Piekarski, B. (2010). Damage of heat-resistant castings in a carburizing furnace. *Engineering Failure Analysis*. 17(1), 143-149. DOI: 10.1016/j.engfailanal.2009.04.011.

[6] Piekarski, B. (2012). *Creep-resistant castings used in heat treatment furnaces.* Szczecin: West Pomeranian University of Technology Publishing House. (in Polish).

[7] Nandwana, D., et al. (2010). Design, Finite Element analysis and optimization of HRC trays used in heat treatment process. *Proceedings of the World Congress on Engineering WCE* 2010. II, 1149-1154.

[8] Bajwoluk, A. & Gutowski, P. (2016). Thermal Stresses in the Wall Connections of Cast Grate Structures. *Archives of Foundry Engineering*. 16(4), 11-16. DOI: 10.1515/afe-2016-0075.

[9] Bajwoluk, A. & Gutowski, P. (2017) The effect of cooling agent on Stress and Deformation of Charge-loaded Cast Pallets. *Archives of Foundry Engineering*. 17(4), 13-18. DOI: 10.1515/afe-2017-0123.

[10] Bajwoluk, A. & Gutowski, P. (2019). Stress and crack propagation in the surface layer of carburized stable austenitic alloys during cooling. *Materials at High Temperatures.* DOI: 10.1080/09603409.2018.1448528.

[11] Bajwoluk, et. al. (2018) Supressing the basket deformation process during heat treatment. Proceeding of 73rd World Foundry Congress. Young Researcher`s Seminar (pp.109-110).

[12] Totten, G.E. (2006). *Steel Heat Treatment*. London: Taylor and Francis Group.

[13] Dossett, J.L., Boyer H.E. (2006). *Practical Heat Treating*. ASM International, 2nd ed.

[14] Lo, K.H. et al. (2009). Recent developments in stainless steels. *Materials Science and Engineering R*. 65, 39-104.

[15] Drotlew, A. et al. (2013). Structure of guide grate in heat treatment technological equipment. *Transactions of foundry research institute*. 53(3), 59-71. DOI: 10.7356/iod.2013.16.

[16] Drotlew, A., Piekarski, B. & Słowik, J. (2017) The design of cast Technological Equipment for Heat Treatment Furnaces. *Archives of Foundry Engineering*. 17(3), 31-36.

[17] Standard EN 10295:2002. Heat resistant steel castings.

[18] Luty, W. (1986). *Quenching cooling agents*. Warszawa: Science-Technical Publishers (in Polish).

[19] Petela, R. (1983). Heat flow. Warszawa: Polish Scientific Publishers, (in Polish).

[20] Hasan, H.S. et al. (2011) Heat transfer coefficient during quenching of steels. Heat Mass Transfer. 47, 315-321. DOI: 10.1007/s00231-010-0721-4.